

# Large Trucks Drag Reduction Using Active Flow Control

Seifert\*, A., Stalnov, O., Sperber, D., Arwatz, G., Palei, V., David, S., Dayan, I., Fono, I.

The Meadow Aerodynamics Laboratory  
School of Mech. Eng., Faculty of Engineering, Tel Aviv University, ISRAEL

## Abstract

Aerodynamic drag is the cause for more than two-thirds of the fuel consumption of large trucks at highway speeds. Due to functionality considerations, the aerodynamic efficiency of the aft regions of large trucks was traditionally sacrificed. This leads to massively separated flow at the lee side of truck trailers, with an associated drag penalty: roughly a third of the total aerodynamic drag. Active Flow Control (AFC), the capability to alter the flow behavior using small, unsteady, localized energy injection, can very effectively delay boundary layer separation. By attaching a compact and relatively inexpensive "add-on" AFC device to the back side of truck trailers (or by modifying it when possible) the flow separating from the truck trailer could be redirected to turn into the lee side of the truck, increasing the back pressure, thus significantly reducing drag. A comprehensive and aggressive research plan that combines actuator development, computational fluid dynamics and bench-top as well as wind tunnel testing was performed. The research uses an array of 15 newly developed suction and oscillatory blowing actuators housed inside a circular cylinder attached to the aft edges of a generic 2D truck model. Preliminary results indicate that a net drag reduction of 10% on full-scale trucks is achievable.

## 1. Scientific background

Active flow control (AFC) is a fast-growing, multidisciplinary science and technology thrust aimed at altering a natural flow state to a more desired flow state (or path). Flow control was simultaneously introduced with the boundary layer concept by Prandtl [1] at the turn of the 20th century. In the period leading to and during WW II, as well as in the Cold War era, flow control was extensively studied and applied mainly to military fluid related systems. Though the fluid mechanics aspect can be robust, steady-state flow control methods were proven to be of inherently marginal power efficiency, and therefore limited the implementation of the resulting systems. Unsteady flow control using periodic excitation and utilizing flow instability phenomena (such as the control of flow separation [2]) has the potential of overcoming the efficiency barrier. Separation control using periodic excitation at a reduced frequency of the same order, but higher than the natural vortex shedding frequency of bluff bodies (such as an airfoil in post-stall or a circular cylinder), can save 90% to 99% of the momentum required to obtain similar gains in performance compared to the classical method of steady tangential blowing. The feasibility of increasing the efficiency and simplifying fluid related systems (e.g., for high-lift, Refs. 7-8) is very appealing. This becomes even more appealing if one considers that *savings of 1%* in the fuel consumption of the US fleet of large trucks (about 5 million trucks) is worth about *\$1.5 billion per year*, while the environmental impact is proportional to the fuel savings. The political implications clearly exist but are difficult to quantify. The progress in the development of actuators, sensors, simulation techniques and system integration and miniaturization enables using wide bandwidth unsteady flow control methods in a closed-loop AFC (CLAFC) manner. (See Ref. 3 for a comprehensive review of the subject.) Experimental demonstrations are required to close the gap between the current theoretical understanding, the computational capabilities and real-world problems. The study described brings together AFC expertise, specifically actuator development and implementation for separation control, closer to real-life industrial applications.

The essential know-how and components of an active separation control system, packaged as an "add-on" device that will be attached to the rear end of large truck trailers, in order to reduce the aerodynamic drag by about 20%, were recently assembled and will be presented in the following sections. At highway speeds, the aerodynamic drag is responsible for roughly 65% of the fuel consumption,

---

\* Corresponding author, [seifert@eng.tau.ac.il](mailto:seifert@eng.tau.ac.il), Associate Prof., Associate Fellow AIAA.

making the potential fuel savings about 10%, taking into account the energy cost of the AFC system. There has been considerable effort in the US to reduce the fuel consumption of trucks using shape changes, simple add-on devices and steady state AFC methods [4], but those have inherent limitations and can lead to only half the expected benefit of our suggested method. Reference 4 cites several research efforts focused on truck trailer drag reduction. Adjustable inclination flat plates could be attached at the truck lee side. These could reduce drag but are rather large, heavy and expensive. Their size raises functionality and compatibility issues. Periodic excitation was also mentioned in Ref 4 but that research effort did not progress far. Steady blowing [10] was also applied to a modified aft region of a truck trailer and resulted in significant aerodynamic drag reduction, but at a marginal to zero or mostly negative energy efficiency due to reasons identified already by our research group [2]. It is expected and substantiated by preliminary CFD analysis and experimental efforts already performed [Sperber et al, 2007], that the combination of steady suction and pulsed blowing could overcome the efficiency barrier discussed.

The current study is aimed at applying active flow control (AFC) technology as an "add-on" device attached to the aft body of heavy trucks and tractor trailer configurations. The TAU-developed Suction and Oscillatory Blowing (SaOB) AFC actuators are used for drag reduction of heavy ground transportation systems. The above fluidic device is a combination of an ejector (jet-pump) and a bi-stable fluidic amplifier that was recently thoroughly studied and the results published by Arwatz et al (2007). The current study is assisted by a computational fluid dynamics (CFD) effort to narrow the huge parameter space. After completing the actuator development and adaptation to the speed range relevant to trucks, three stages of experiments were performed on a circular cylinder, the generic bluff-body (see Sperber et al, 2007). These studies resulted in a significant reduction of drag due to delay of boundary layer separation. A wide range of boundary conditions were tested and only the common results to all conditions were considered as valid. Successful wind tunnel demonstration on a two-dimensional (2D) equivalent of a blunt truck trailer model was subsequently performed and is the main subject of this paper. This stage is to be followed by a complete, small-scale, truck model with drag reducing devices and a full scale prototype of the "add-on" device for road testing will follow. The technology could lead to a revolutionary aerodynamic drag reduction of heavy road vehicles and could lead to new efficiency levels of aeronautical systems as well. The current research is especially appealing since it provides a valuable contribution to a slower production of greenhouse gases and a significant reduction of other emissions.

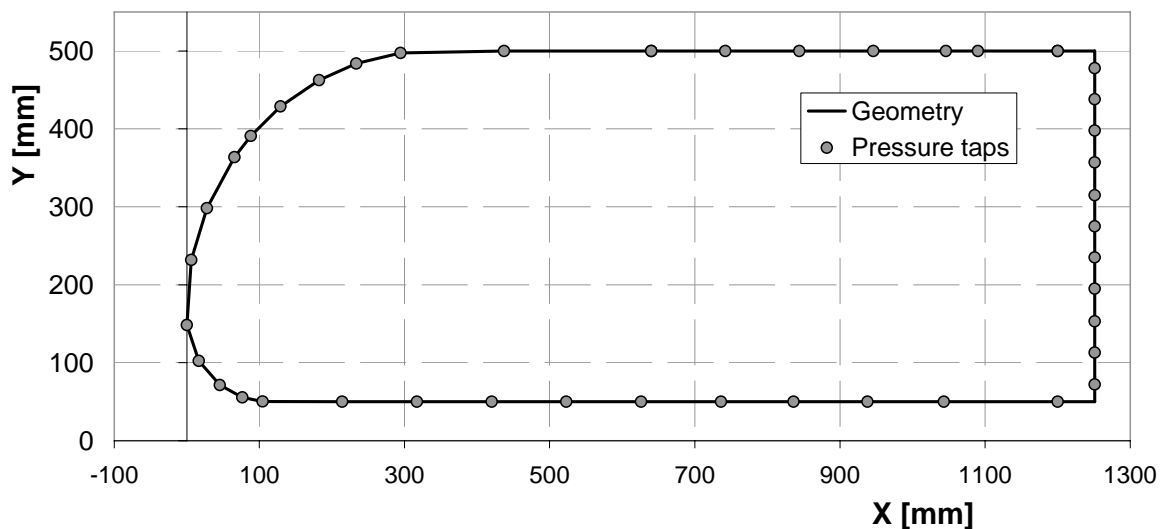


**Fig. 1** A cross section of the 2D “truck” model,  $H=450\text{mm}$ ,  $L=1250\text{mm}$  and its width,  $b=609\text{mm}$ . No control cylinders.  $Y=0$  is the simulated road level, when present.

## 2. Description of the experiment

The experiments were performed on a generic 2D equivalent model of a large truck, along the lines of the GTS model [Ref. 15]. Figure 1 presents a cross section of the model, showing also the location of the 43 pressure taps. The model height ( $H$ ) is 450mm and its length is 1250mm. It spans the entire width of the wind tunnel test section,  $b=609\text{mm}$ . The model is made of aluminum beams and ribs and a skin of 2mm

thick aluminum plates. The significant interference with the wind tunnel has not been taken into account in any manner. However, during the 2D truck experiments the ceiling static pressures were measured and could be used for evaluation of the wind tunnel interference with the use of future CFD effort. It is argued that since the flow accelerates more around our model, with respect to free flow conditions, the AFC results are conservative since the AFC effects are proportional to the flow linear momentum at the separation points. For control purposes, one or two circular cylinders were attached to the aft region of the truck model. The cylinders were 76.2mm in diameter and spanned the 609mm of the wind tunnel. The cylinders were installed so that they were tangent to the aft body corners and extended one radius behind the aft plate line, their centers one radius below the upper cover plate or above the lower cover plate, respectively. See Fig. 7a with only the upper control cylinder sketched. The upper control cylinder was installed with an array of 15 SaOB actuators, as described in Sperber (2007) and Sperber et al (2007). An array of 96 suction holes with diameter of 2mm and spacing of 6mm were drilled in the cylinder. The wall thickness was close to 10mm, so the flow resistance was high. The flow was sucked into the cylinder by the ejector which is part of the SaOB actuator array. The entire flow rate (the sum of the inlet and entrained-sucked flow) was ejected alternatively out of two tangential, 1.7mm high, pulsed blowing slots connected to each actuator. Each actuator was 28mm wide and it controlled about 40 mm of the span of the cylinder. The lower control cylinder was used only for steady-suction and was connected to an external suction pump. It had two staggered rows of 96 holes 2mm diameter each, spaced 7.5 deg apart along the cylinder arc (Figs. 10a and 10b).

A simulated road was placed under the 2D truck in some of the tests. The plate was positioned 67 cm upstream of the model and was 280 cm long, 4mm thick, extending 90 cm behind the model. A 3D wake rake was positioned 120 cm downstream of the model. It measured 29 total pressures and 2 static pressures, one close to each sidewall. The wake rake was mounted on a Y-axis traverse allowing vertical motion, with typical resolution of 20–25mm.

The experiments were performed in the Meadow-Knapp low-speed wind tunnel. The speed range is 4–60m/s, the turbulence level is about 0.1% and the test section dimensions are 1.5m (high) by 0.61m (wide) and 4.25m long. Pressures were measured by a PSI Inc. pressure scanner with 128 ports at a resolution of 0.001psi. Tunnel dynamic pressure was measured by a Pitot-Prandtl tube, positioned 110cm upstream of the model leading edge on the tunnel ceiling, connected to a Mensor pressure transducer (10" water full scale and resolution of 0.06%). The Reynolds number was monitored to 1% tolerance and unsteady pressures were also measured on the model aft region, to identify unsteady effects. The tunnel temperature was  $24 \pm 2^\circ\text{C}$ . Air density and viscosity were calculated using standard formulae and the ambient temperature and pressure.

### 3. A brief review of recent related work

#### a. Suction and Oscillatory Blowing (SaOB) Actuator

The development of the SaOB actuator (Arwatz et al, 2007) and its utilization for drag reduction on the circular cylinder (currently used as the aft-upper control device), were reported elsewhere (Sperber, 2007 and Sperber et al, 2007). However, for the sake of completeness and due to the time-lag until these studies become publicly available, some of the results are cited and discussed here.

The Tel Aviv University (TAU) suction and oscillatory blowing (SaOB) actuator was invented in October 2003, patented [5] and it was the subject of a recent two-year study. Several size actuators were developed. A theoretical model for the valve operation was validated (Arwatz et al, 2007). Small size devices, suited for the current application with minor adjustments, were also developed and validated (Sperber, 2007, Sperber et al, 2007). A cross-section of the actuator can be seen in Fig. 2a and a sketch explaining the principle of operation is shown in Figs. 2b and 2c. The actuator is a combination of a bi-stable fluidic oscillator connected downstream of an ejector ("jet pump"). The purpose of the ejector is to create a suction flow, by increasing the flow entrained into the valve. Suction is probably the most efficient flow separation control method [9], but is difficult to generate efficiently. It has been shown that the ejector is indeed increasing the flow rate by a factor up to three with its entrances unrestricted. To create self-oscillations, the two control ports (Figs. 2a and 2c) were connected by a short tube, without any moving part or energy expenditure. The tube was later replaced by an S-shaped channel machined in a plate on which all the actuators were installed (referred hereafter as "mounting plate"). The SaOB actuator has a wide and appropriate frequency range (0.1 to 1.4 kHz) depending on the ejector nozzle shape, the length of the feedback tube and the inlet flow-rate (Arwatz et al, 2007). Near-sonic actuator exit velocities

have been measured, but currently the exit velocities are of the same order as the free-stream velocities. The inlet flow rate is controlled by a pressure regulator connected to shop air supply - to be replaced by the truck pneumatic system - by flow extracted from the truck turbocharger or by an auxiliary system connected electrically to the truck alternator or mechanically to the rear wheels. The valve operation is insensitive to rain or dust conditions.

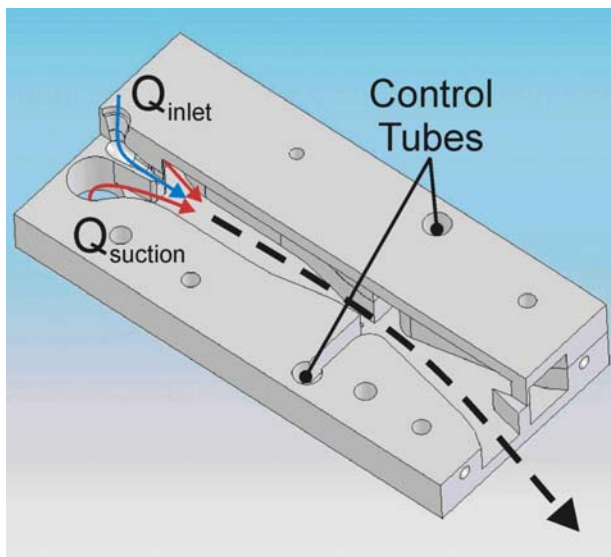


Fig. 2a Small size suction and oscillatory blowing actuator. Overall length is about 60mm.

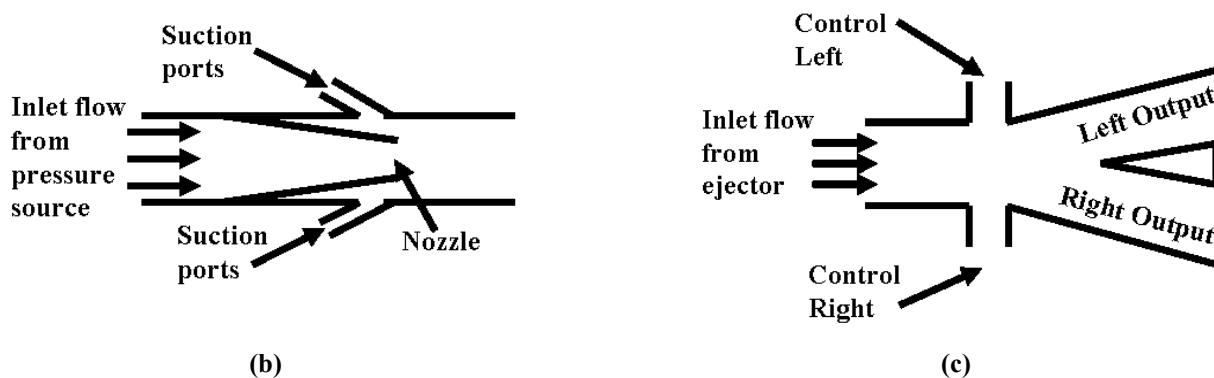


Fig. 2b,c: A schematic rendering of the SaOB actuator: (b) ejector (c) switching valve.

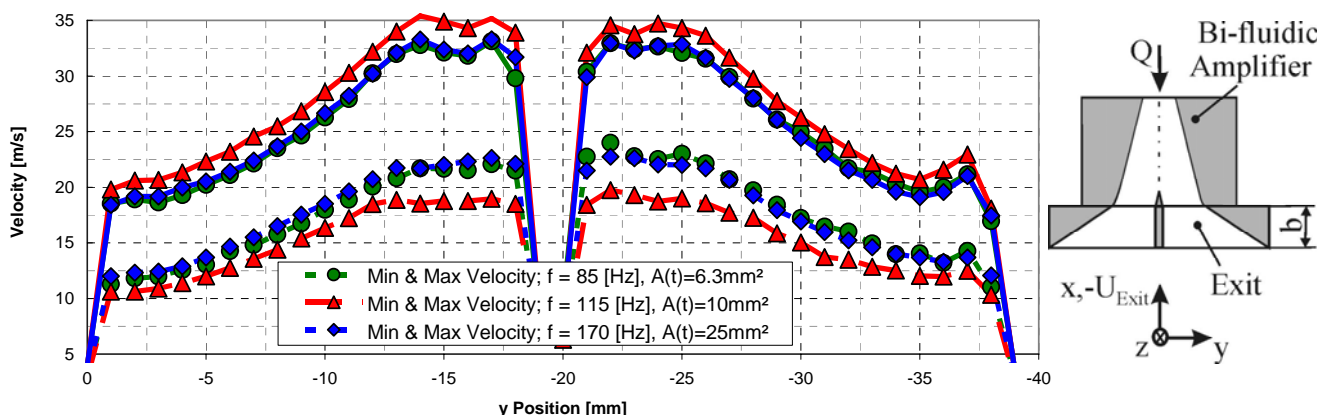


Figure 3: Valve exit velocity profiles for three different feedback-tube diameters (maximum velocity = solid lines; minimum velocity = dashed lines;  $p_{(inlet)}=6$  [psi]) measured with Hot-Wire-Anemometry; (right) Slot configuration drafted. Length of control tube, 80mm.

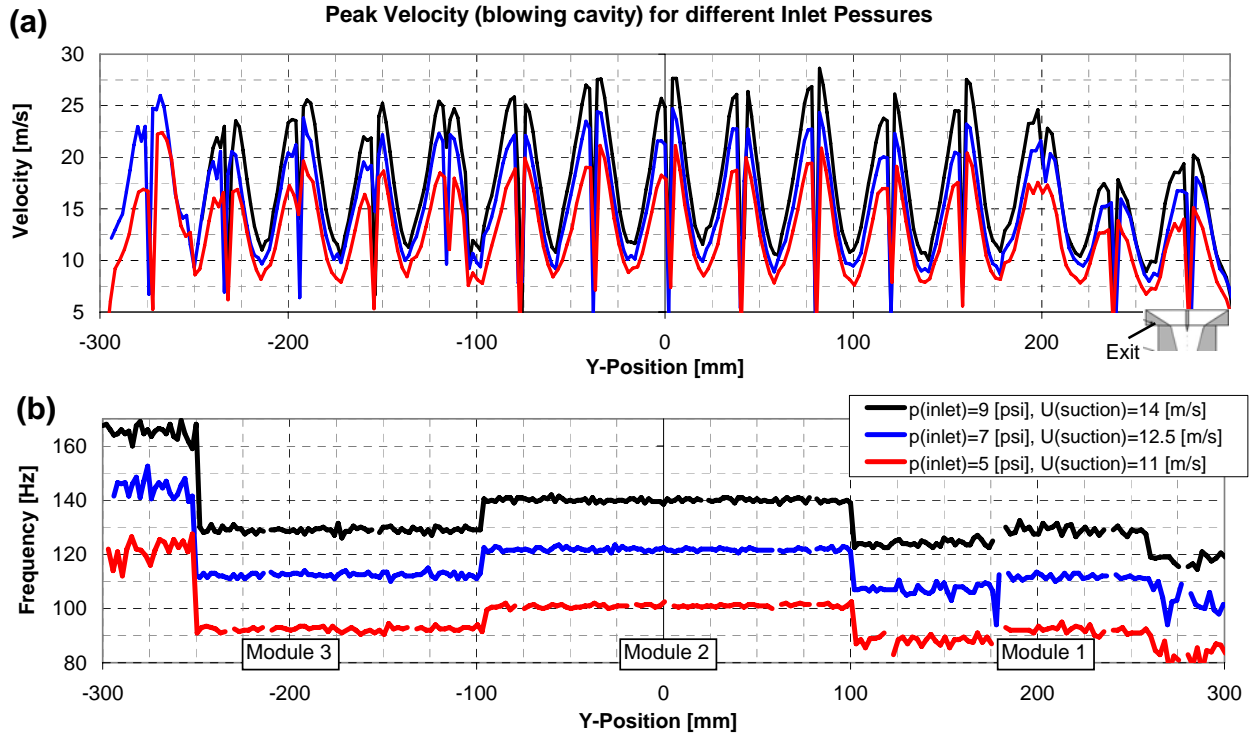


Fig. 4 Measurement of the output of a 14-valves array installed in a circular cylinder. (a) velocity, (b) frequency.

During the course of the study reported by Sperber et al (2007), there were several cycles of modifications to the valve design. The main objective was to fit the valve into the cylinder while minimizing the pressure drop across it. This was achieved by redesigning the ejector nozzle to have a short converging straight geometry and shortening the mixing chamber between the ejector and the oscillator to the minimum possible (Fig. 2a).

Following these modifications the valve was bench-top tested, initially only with exit restrictions, simulating the assembly in the control cylinder. Figure 3 shows the maximum and minimum flow velocity out of a single SaOB actuator with an exit assembly simulating the conditions that will prevail in the "add-on" device as well as in the control cylinder at half scale. The exit velocities were measured by a hot wire that was traversed along the exit slot. The cross-section of the feedback tubes (all with  $L=80\text{mm}$ ) was altered during those tests. It can be seen that the cross section of the feedback tube has a strong effect on the oscillation frequency. It has a weaker effect on the switching quality, defined as:  $\kappa = \frac{U_{\max} - U_{\min}}{U_{\text{average}}}$ .

### b. Circular Cylinder with the SaOB Actuator Array

The 15-valve array was mounted on a plate, providing inlet pressure to all the valves, feedback for each valve self-oscillation, and synchronization tubes between the valves. The cross section of the feedback tubes was  $5.7\text{mm}^2$  and their length was maintained at 80mm. The reader is referred to Sperber et al (2007) for more details. Figure 4 shows the velocity (a) and frequency (b) of oscillation of an actuator array installed in the circular cylinder and tested on the bench-top set-up. The valves were not all synchronized, the frequencies of the central 13 valves deviated by no more than 10%, and the peak velocities deviated by a maximum of 20%. These results seemed sufficient to go ahead and test the valve array for the purpose of the cylinder and later the 2D truck model drag reduction, while it is planned to continue improving the uniformity of the magnitude and frequency and the synchronization between the different valves.

The combination of oscillatory-blowing and steady-suction has never been tested before this project, but both methods are known to be very effective for the control of boundary layer separation [3]. A significant body of knowledge has been acquired by Sperber et al (2007). These experiments established the drag reducing capability of steady-suction through a 2D slot and later a row of holes in a

wide range of boundary conditions. The data set also established that a 15 deg delay in separation region on the circular cylinder at  $Re=100,000$  and  $Re=150,000$  (associated with the target highway driving speeds for the current cylinder diameter) is possible with suction magnitude of about half the free-stream velocity. This enabled the definition of the configuration shown on the right side of Fig. 5. The suction holes are located 15 deg upstream of the pulsed blowing slot. The array of 15 SaOB actuators is mounted inside the 76.2mm diameter cylinder. Inlet flow is provided via common channel feeding all the ejectors' jets. These create low pressure in the half-cylinder to the left of the valve array, sucking flow through the holes. The entire flow is then ejected through the pulsed blowing exit slots. The oscillation frequencies are in most cases larger than the natural vortex shedding frequencies on a circular cylinder at the current velocity range and significantly higher than the 2D truck model vortex shedding frequency. Three series of wind tunnel experiments were performed on the circular cylinder (shown in Fig. 5, Sperber et al, 2007).

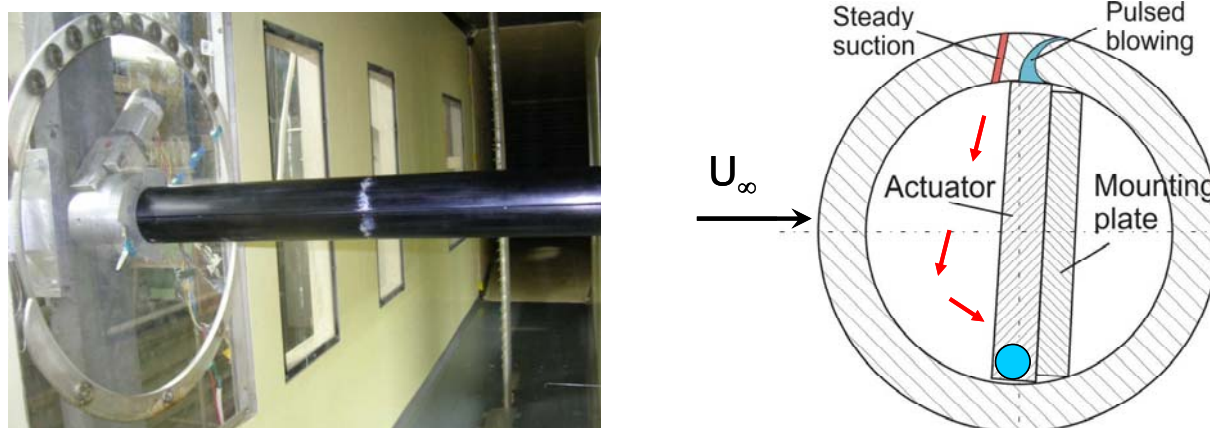


**Figure 5: A sketch of the cylinder Setup (right) with the suction holes (red) and the tangential slot (light blue) installed at the Meadow-Knapp Wind Tunnel (left). An array of 15 SaOB actuators was installed in the cylinder. The sketch on the right also shows the mounting plate for synchronization and pressure supply (right, light blue circle). The arrows indicate the path of the suction flow. Fig. 2a shows the sucked flow entrance to the valve, not shown above.**

Figure 5 shows the experimental set-up of the cylinder in the Meadow-Knapp wind tunnel and a cross section of the 15-valves actuator array as installed inside the cylinder.

The cylinder was tested and a sample of the drag reduction data is presented in Figure 6 below.

The data shown in Figure 6 indicates a drag coefficient reduction from about 1.1 to about 0.7, or a relative drag reduction of about 35%. This is obtained when the suction holes are located at about 110 deg (relative to the free-stream direction) on the cylinder and the pulsed blowing slot at are positioned 15 deg downstream (at about 125 deg), where 90 deg is the summit of the cylinder. The energy efficiency of this drag saving, which was measured at flow speed comparable to the highway speed of trucks, indicates net positive energetic efficiency (Sperber et al, 2007). For the acquisition of all the data presented below, net energy efficiency was the prime consideration. As shown in Fig. 7a, the add-on device will have a shape that resembles a semi- to quarter-cylinder attached to the back side of a truck trailer. The advantage of having a complete cylinder at this stage of the study is the capability to conveniently alter the actuation location, which is shown to be very sensitive on the free cylinder (Fig. 6) and also in the results related to trucks, presented later in the paper.

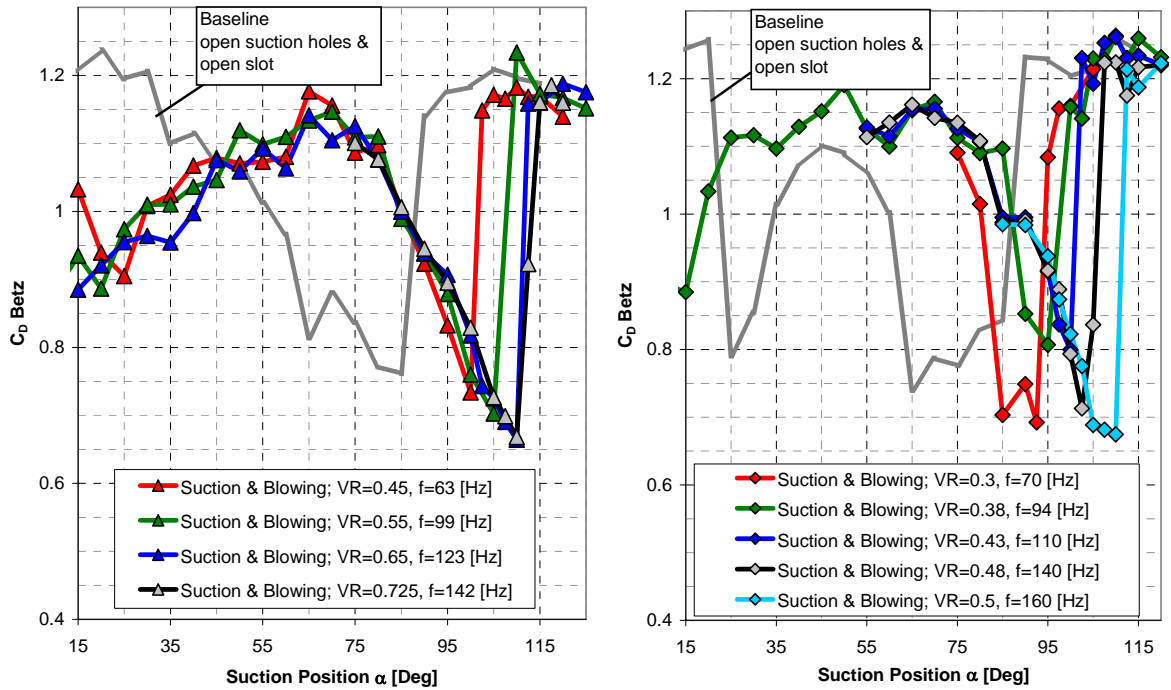


**Figure 6: Cylinder drag coefficient ( $C_D$  Betz) versus Suction Position (0 deg is the front stagnation point of the cylinder) in “free” (no truck model) laminar flow conditions; measured with steady-suction and oscillatory-blowing actuation for two Reynolds numbers and different amplitudes (left)  $Re_d=100k$  (right)  $Re_d=150k$ , the pulsed blowing slots are located  $\Delta\alpha=15$  deg downstream to the suction holes. VR is the velocity ratio between the suction and free-stream velocities.**

#### 4. Two-dimensional (2D) truck experiments

##### a. Two-dimensional (2D) truck with SaOB cylinder at upper aft corner

Figure 7a shows a schematic cross-section of the 2D truck model, with the SaOB cylinder installed on its upper aft corner. Figures 7b and 7c present pictures of the model installed in the Meadow-Knapp wind tunnel, above a simulated road. The vertical distance between the model and the floor was allowed to increase from 50 to 55mm in order to compensate for boundary layer growth. It was validated that the boundary layers did not restrict the free flow under the model. Wheels or a moving floor were not used. These effects seem secondary since most of the effort was spent on the upper aft corner, least effected by the wheels or simulated road, moving or stationary. However, the mere presence of the simulated road is essential for simulating a side view of the truck driving on a road. Several 50mm wide roughness strips (grit #60) were placed on the top and bottom plates of the 2D truck model, to reduce Reynolds number effects. Figure 7d presents a close-up view of the upper aft control cylinder. An array of 96, 2mm diameter, holes was positioned 15 deg upstream of a 1.7mm (nominally) wide slot. The slots allowed almost tangential downstream-directed introduction of the pulsed blowing excitation. Each actuator controlled a span of about 40mm with two exits, as shown schematically in the insert of Fig. 3. The trailing edge of the top and bottom cover plates were machined to create a back-step no thicker than 0.5mm, allowing a smooth transition of the flow from the covers to the control cylinders.

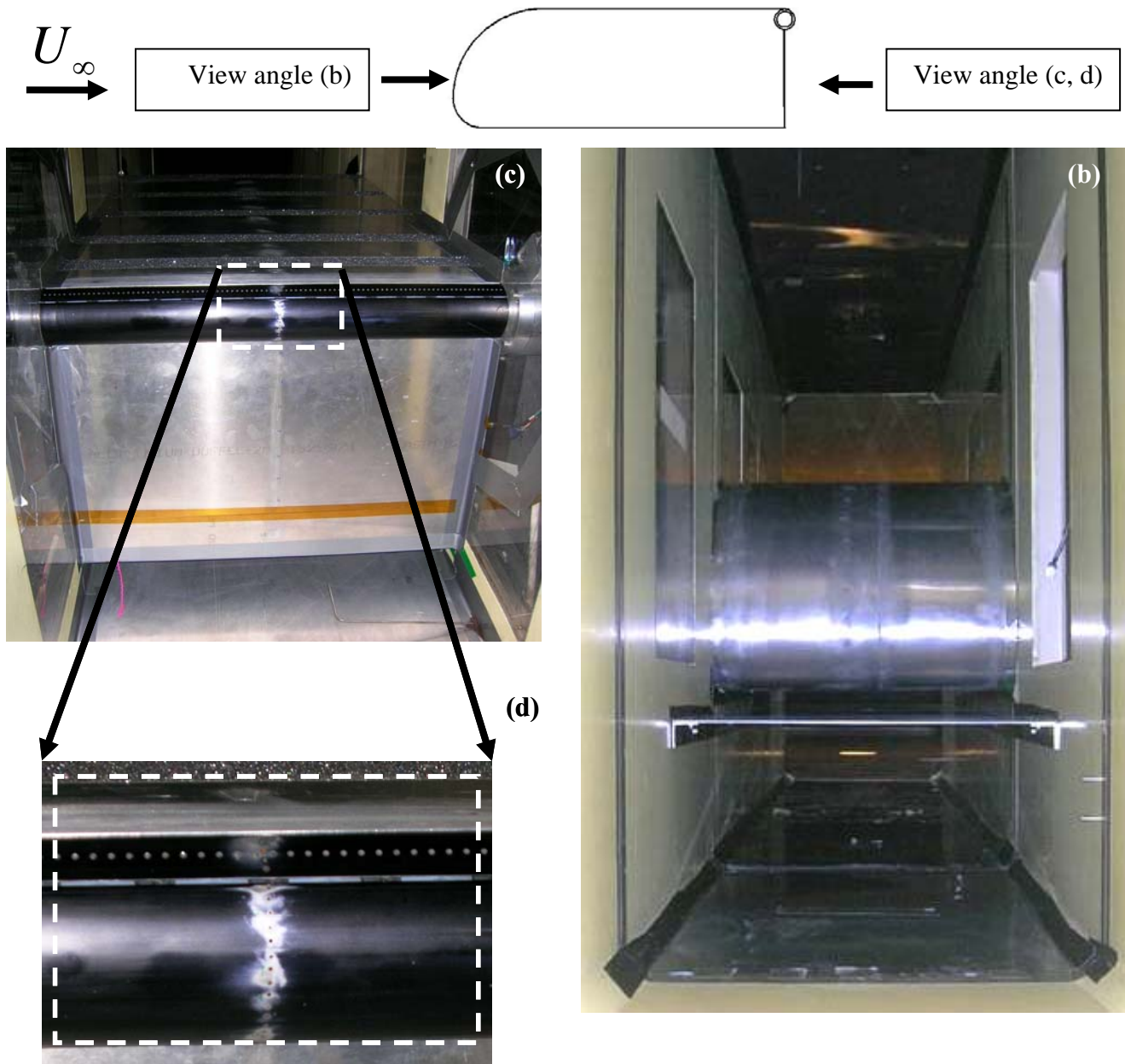


**Fig. 7 The 2D truck model: (a) cross-section (flow is coming from left to right); (b) front-view showing the model installed in the tunnel 50-55mm above the simulated road; (c) a rear-view showing the back plate and SaOB instrumented cylinder on the top-rear edge; and (d) close-up of the row of 96, 2mm diameter suction holes and 1.7mm wide pulsed blowing slot on the cylinder (that was allowed to rotate for optimal positioning of the actuation locations).**

Of major importance was the determination of the optimal holes/slot location. Note that at this stage of the investigation the angular distance between the suction holes and pulsed blowing slots was fixed, 15 deg, based on the results of Sperber et al, (2007).

The drag of the 2D truck model was calculated from the integration of the pressures around the model and from a 3D wake survey performed 1.2m behind the model. The wake flow was found to be reasonably 2D and the agreement between the two methods of drag evaluation was better than 2% in most cases, and in the absence of the simulated road. The drag reduction magnitudes were similar when evaluated either with the wake integration method or from the pressure drag. The aft body "add-on" device was tested as a circular cylinder, due to the larger size and ease of installation of the 15 SaOB

valve array inside it. A secondary major consideration was the capability to rotate the cylinder, bringing the holes/slot to an optimal location.

Figure 8a shows the form-drag of the 2D truck model with the SaOB cylinder installed at the upper aft corner. The addition of the passive control cylinder at the upper aft corner had a drag reducing effect of about 5% with respect to the baseline configuration shown in Fig. 1. The slot was just exposed when its location was 90 deg. With the control cylinder present but when the slot was hidden,  $C_{dp}=0.99\pm 0.01$ . The passive effect of the slot, and its associated discontinuity, can be seen by the drag increase between 90 and 100 deg. At larger slot locations the drag returns to its undisturbed value, with a possible drag penalty of 0.01–0.02. At slot positions greater than 105 deg both slot and suction holes are exposed. Fig. 8 also shows results of different levels of control applied by the array of SaOB actuators, with increasing level of input pressures, as indicated in the legend. A significant drag reduction develops in the range of tested pressures, up to 0.05MPa. An optimal holes/slot location can be identified around 130–132.5 deg, slightly increasing with the magnitude of the control authority. These results were obtained with a simulated road, similar to a truck with control applied only from the top aft edge of the trailer. It was later found that adding a second control cylinder at the lower aft edge, *with simulated road* did not provide additional drag reducing effect.

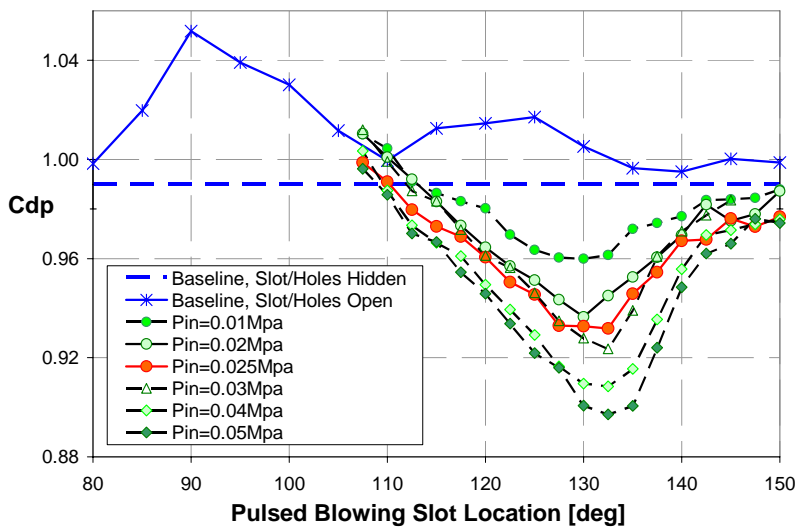


**Fig. 8a** The effect of the SaOB actuation on the drag of the 2D truck model at  $U=25\text{m/s}$  for different actuation levels indicated by the inlet pressures. The actuation location is altered via cylinder rotation, where 90 deg is the cylinder – upper plate junction.

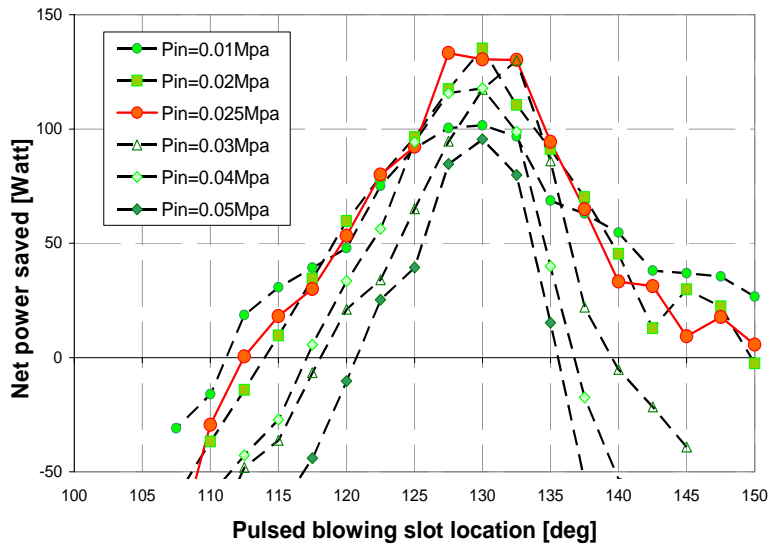


**Fig. 8b** The effect of the SaOB actuation on the required power to propel the 2D truck model at  $U=25\text{m/s}$  for different actuation levels indicated by the inlet pressures. The actuation location is altered via cylinder rotation, where 90 deg is the cylinder – upper plate junction. Reference power is about 2.57kWatt.

Despite the apparent capability of increased levels of SaOB inlet pressure to provide further drag reduction, one should consider the energy cost of the control input, since our aim is a reduction in *fuel consumption* and therefore total invested power should be a prime consideration. The net power saving was calculated according to:  $Power\ saved = 0.5\rho U_\infty^3 S\Delta C_d - P_i Q_i / \eta$ . Where  $\rho$  is the air density,  $U_\infty=25\text{m/s}$  is the free-stream velocity,  $S=0.61\times 0.45\text{m}^2$  is the 2D truck cross-section area,  $\Delta C_d$  is the drag reduction at the same holes/slot position with respect to the baseline uncontrolled condition. The control power was taken as the product of the inlet pressure ( $P_i$ , measured at the supply line) and the inlet flow rate ( $Q_i$ , measured by an orifice flow meter at the pressure regulator and neglecting the effect of the larger static pressure on the flow rate, making the actual flow rates smaller by 5–20% than those currently cited depending on the excess pressure). The pumping efficiency,  $\eta$ , was taken as 75%, as in many common low-pressure compressors. In reality the control flow was provided by the lab shop air through a computer controlled pressure regulator. The data presented in Fig. 8b shows a rather insensitive (to the inlet pressure) peak power saving of around 130 watts for inlet pressures of 0.02–0.025MPa. With either lower or higher pressure levels, the power efficiency decreases.

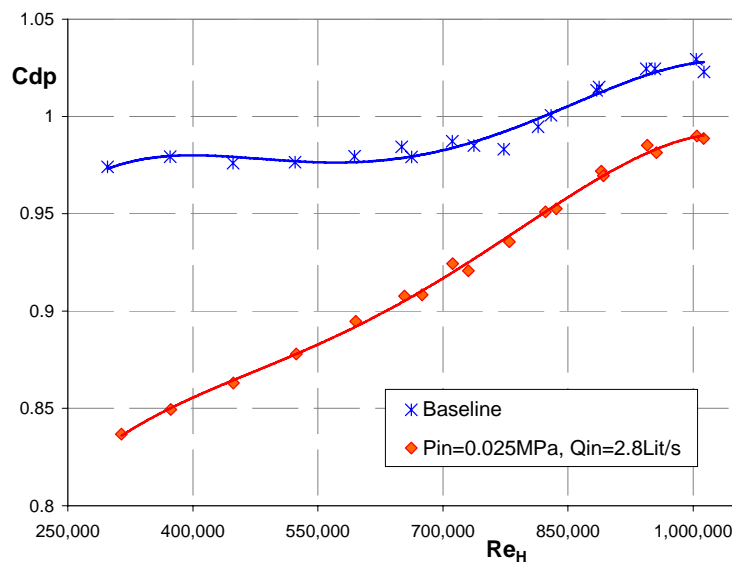


**Fig. 9a** The effect of the SaOB actuation on the baseline and controlled drag of the 2D truck model vs. the height Reynolds numbers for fixed actuation level. The actuation location is: pulsed blowing slot at  $\alpha=130^\circ$ , suction holes at  $\alpha=115^\circ$ ,  $P_{in}=0.025\text{ MPa}$ ,  $Q_{in}=2.8\text{ Lit/s}$  where 90 deg is the cylinder – upper plate junction.

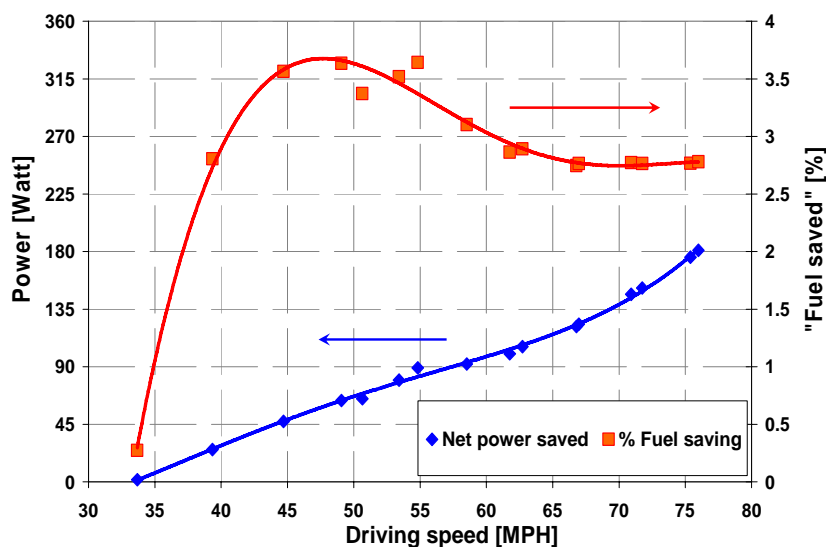
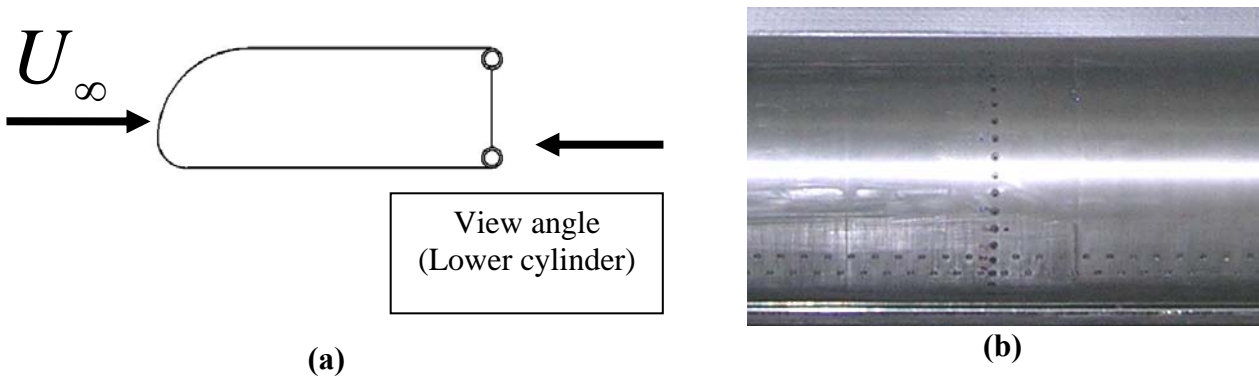


**Fig. 9b** The net flow power saved and equivalent “fuel” saving of the controlled 2D truck model vs. the driving speed for fixed actuation level. The actuation location is: pulsed blowing slot at  $\alpha=130^\circ$ , suction holes at  $\alpha=115^\circ$ ,  $P_{in}=0.025\text{ MPa}$ ,  $Q_{in}=2.8\text{ Lit/s}$  where 90 deg is the cylinder – upper plate junction.

While the data presented in Figure 8 was obtained at a fixed free-stream velocity of 25m/s, it is important to evaluate the effectiveness of the drag reducing technology over the entire range of free-stream velocities, or driving speeds. Furthermore, this was done with one actuation condition, allowing, for simplicity, the system to be turned on or off with no proportional control. Figure 9a presents form-drag data for the 2D truck model, with one upper control cylinder, the SaOB array installed on the upper aft edge of the 2D truck model (as shown in Fig. 7a). The simulated road was present in this experiment. The drag slightly increases, from 0.98 to 1.02 with Re (based on the model height and the free-stream velocity) increasing from about 200,000 to about 1,000,000. Note that at the larger Re range the drag reaches a plateau. This Re, based on the height of the model, is considered minimal for Reynolds number free results. With fixed level of inlet pressure and fixed actuation locations, as indicated in the legend and caption of Fig. 9a, one can clearly note a significant drag reduction over the entire Re range. It is only natural to expect that the magnitude of the drag reduction will decrease as Re increases, due to the relative decrease between both the suction and pulsed blowing magnitudes when normalized by the free-stream velocity. Clearly, aerodynamic drag reduction of about 20% is possible at low speeds, decreasing to about 5% at the highest speeds considered operational and legal for large trucks in the US highway system.

While the drag reduction is of interest, net power efficiency is our prime target. Figure 9b shows the net power saved and the percentage of net power saving. The latter is equivalent to about twice the expected fuel saving after considering friction resistance and wind averaged performance. One can note a 45-watt power saving at 45MPH increasing to 180 watts saved at 75MPH. These power savings translate to more than a 3.5% power saving at speeds between of 45–55MPH. At higher speeds the aerodynamic power saving (taking into account the invested power in the actuation system) saturates at about 2.8%. Considering that at these speeds (above 60MPH) two thirds of the power is invested in overcoming aerodynamic drag, the equivalent net fuel savings is about 1.9%. While these numbers might appear small, they are still significant. The inlet pressure was optimal at about 50MPH, so larger control authority would shift that peak to higher speeds, depending on the target speed range. Furthermore, the obtainable drag reduction due to the application of the control on the upper aft edge with the simulated road present is smaller compared to its application on the sides of the truck, as will become clear from the subsequent discussion.

**b. Two-dimensional truck with two control cylinders**



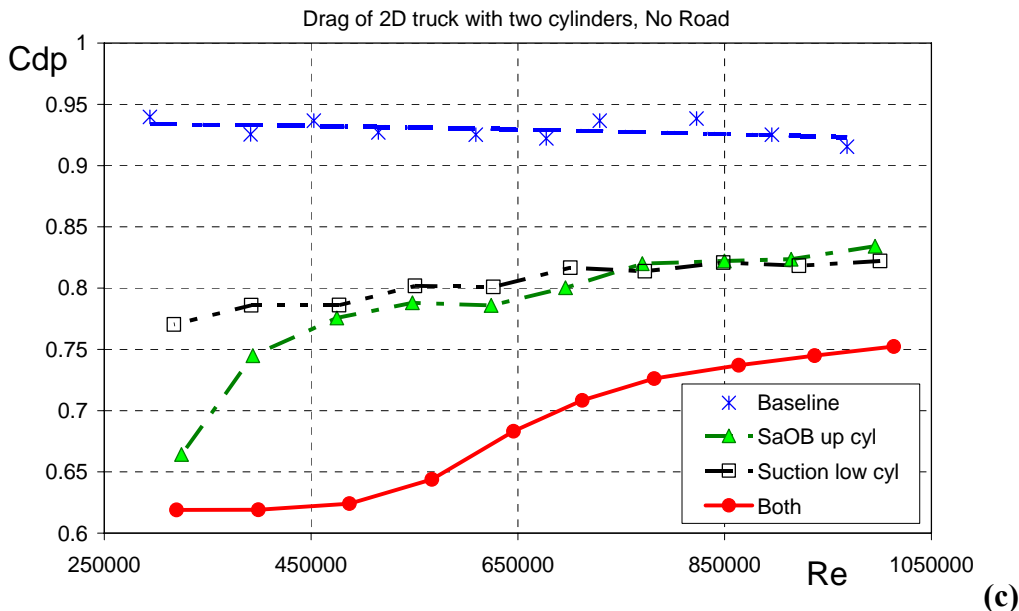


**Fig. 10 (a)** A sketch of the 2D truck model with two control cylinders, **(b)** a close-up rear-view of the lower aft-corner control cylinder, and **(c)** drag reduction due to SaOB array on top aft, Suction cylinder on bottom aft corners. The actuation locations are: pulsed blowing slot at  $\alpha=130^\circ$ , suction holes at  $\alpha=115^\circ$ ,  $P_{in}=0.04$  MPa, where  $90$  deg is the cylinder summit. Lower cylinder: two rows of suction holes, the 1<sup>st</sup> at  $\alpha=-121^\circ$ , the second at  $\alpha=-128.5^\circ$ . Lower cylinder suction magnitude was tuned to provide the same drag reduction as the SaOB array alone at  $Re\sim 800,000$ . In **(c)**, form-drag coefficient vs. Reynolds number for four states: baseline, only the upper SaOB cylinder is turn on, only the lower suction cylinder is on, and both control cylinders are on.

To assess the effectiveness of controlling both vertical sides of the aft truck trailer, the simulated road was removed and a second control cylinder was mounted on the lower aft edge of the 2D truck model, as shown in Fig. 10a. The lower control cylinder was also mounted on a rotary system to allow optimal control locations. However, for simplicity, cost and time considerations only steady-suction was applied at the lower control cylinder. It should be noted that suction only (lower cylinder) is not as effective as SaOB actuation (upper cylinder). Detailed comparison of the effectiveness of the two control methods (with suction only and with the SaOB valve array) can be found in Sperber et al (2007) for an isolated cylinder. The suction was applied from two rows of staggered 2mm diameter holes, each containing 96 holes and spaced  $7.5$  deg in their angular locations (seen in Fig. 10a as well). The lower suction holes were just exposed for holes location of  $-90$  deg. The same optimization procedure was applied to the lower cylinder, as previously applied to the upper control cylinder, in order to identify a condition which provides the same level of drag reduction that the upper SaOB control cylinder is capable of with inlet pressure of 0.04 MPa. This higher pressure level was selected based on the results shown in Figs. 8 and 9 and discussed above.

The data presented in Fig. 10b shows that the baseline drag of the 2D truck model, with two control cylinders and without the simulated road is  $0.93\pm 0.01$  regardless of the Reynolds number. The two control cylinders, when operated alone, can provide significant and similar drag reduction over the entire  $Re$  range, with the exception of the SaOB control that is more effective at low speeds. This difference might be associated with the oscillation frequency being somewhat low, and therefore optimal at low speeds. When the two control cylinders operate together, a very encouraging trend can be noted, i.e., that the drag reducing effects accumulate. The data presented in Fig. 10b demonstrates about 20% aerodynamic drag reduction at highway speeds, translated to about 10% net fuel savings on large trucks, busses, and tractor trailer configurations.

A smaller 3D truck model with an array of SaOB actuators is currently being tested. Road tests will hopefully be conducted during the second quarter of 2008.

## 5. Conclusions and recommendations

A comprehensive set of experiments were conducted with the aim of reducing the aerodynamic drag of large trucks by 20%. This effort included: (1) development, modeling and adjustment of the SaOB actuator to low-speed operation, (2) installation of a 15-valve actuator array in a circular cylinder, (3) comprehensive wind tunnel testing of the drag reduction effects on the circular cylinder under the effect of various boundary conditions, (4) the design and testing of a 2D truck model with and without simulated road, with and without control cylinders, and finally, (5) evaluation of the energy efficiency of control cylinder(s) drag reducing capability. Only stages (4) and (5) are currently discussed. Two related publications (Arwatz et al, 2007, Sperber et al, 2007) discuss stages 1 through 3.

It was found that the optimal location for introducing the suction through holes is about 15–20 deg downstream of the plate-cylinder junction. During the cylinder-alone tests, it was found that suction with half the free-stream magnitude is capable of 15 deg separation delay. Therefore, the pulsed blowing was introduced 15 deg further downstream of the suction holes. One control cylinder positioned at the upper aft edge of the simulated trailer is capable of about 10% drag reduction. But if the power invested in the actuation is considered, the optimum is obtained at lower fluidic power input, where the aerodynamic drag reduction is roughly 6–7%. When two control cylinders were applied in a situation simulating a control applied to the two vertical edges of the aft-trailer region, a 20% drag reduction is possible. This should lead to at least 10% net fuel savings on a full scale truck.

Significant enhancement in power efficiency is expected when scale-up of the small-size model will be performed. This power efficiency enhancement should originate from lower resistance of the suction holes (due to larger diameter, smaller wall thickness and rounded edges) and a factor of 2-4 power saving on the actuators' ejector due to the larger ejector nozzle cross section.

## 6. Acknowledgment

The authors would like to thank the lab leading technician S. Pastuer for the superb support. To T. Bachar, to our previous lab engineer Mr. E. Ben-Hamou, to our lab technicians: A. Blas, A. Kronish, S. Balvis, S. Moshel and to the lab electric and computers engineer M. Vaserman for the great technical support.

The research was funded by the Yeshaya Horowitz Fund and managed by RAMOT of Tel Aviv University. Three patents (one approved and two pending) exist.

## 7. References

1. Prandtl, L., "Motion of Fluids with Very Little Viscosity", Third International Congress of Mathematicians at Heidelberg, 1904, from Vier Abhandlungen zur Hydro-dynamik und Aerodynamik", pp. 1-8, Gottingen, 1927, NACA TM-452, March 1928.
2. Seifert, A., Darabi, A. and Wygnanski, I., 1996, "Delay of Airfoil Stall by Periodic Excitation", J. of Aircraft. Vol. 33, No. 4, pp. 691-699.
3. Collis, S.S., Joslin, R.D, Seifert, A. and Theofilis, V., "Issues in active flow control: theory, simulation and experiment", Prog. Aero Sci., V40, N4-5, May-July 2004 (previously AIAA paper 2002-3277).
4. Annual Progress Report for Heavy Vehicle System Optimization, Feb. 2005, US Dep of Energy. see: [http://www.eere.energy.gov/vehiclesandfuels/pdfs/program/2004\\_hv\\_optimization.pdf](http://www.eere.energy.gov/vehiclesandfuels/pdfs/program/2004_hv_optimization.pdf)
5. Seifert, A., Paster, S., "Method and mechanism for producing suction and periodic flow", US Patent 2006-0048829-A1, Granted 2005.
6. Arwatz, G., Fono, I. and Seifert, A., "Suction and Oscillatory Blowing Actuator", paper presented in the MEMS IUTAM meeting, September 2006, London, UK.
7. Pack Melton, L.G., Schaeffler, N., Yao, C.S. and Seifert, A., "Active Control of Flow Separation from the Slat Shoulder of a Supercritical Airfoil", J. of Aircraft, 42 (5): 1142-1149 SEP-OCT 2005 (previously AIAA Paper 2002-3156).
8. Pack Melton, L.G., Yao, C.S. and Seifert, A., "Active Control of Flow Separation from the Flap of a Supercritical Airfoil", AIAA J., 44 (1): 34-41 JAN 2006 (previously AIAA Paper 2003-4005).
9. Seifert, A. and Pack, L.G., "Active Control of Separated Flow on a Wall-mounted "Hump" at High Reynolds Numbers", AIAA J., V. 40, No. 7, July, 2002, pp. 1363-1372. (Part of AIAA paper 99-3430).

10. Englar, R.J., Advanced aerodynamic device to improve the performance, economics, handling and safety of heavy vehicles, SAE paper 2001-01-2072
11. Englar, R.J., Pneumatic Aerodynamic control and drag reduction system for ground vehicles, US patent 5,908,217, June, 1, 1999.
12. Arwatz, G., Fono, I. and Seifert, A. "Suction and oscillatory Blowing Actuator", AIAA J. 2007, to appear.
13. Sperber, D., Dipl. Eng. Thesis, TUB and TAU, 2007.
14. Sperber et al, "Drag reduction of a circular cylinder at transitional Reynolds numbers", to be published.
15. R.C. McCallen, K. Salari, J. Ortega, L. DeChant, B. Hassan, C. Roy, W.D. Pointer, F. Browand, M. Hammache, T.Y. Hsu, A. Leonard, M. Rubel, P. Chatalain, R. Englar, J. Ross, D. Satran, J.T. Heineck, S. Walker, D. Yaste, B. Storms, "DOE's Effort to Reduce Truck Aerodynamic Drag-Joint Experiments and Computations Lead to Smart Design" AIAA paper June 2004.